

https://dspace.org/

# Characterization and performance evaluation of angularshaped fly ash aggregates for pavement base and subbase applications

**Hrishikesh Shahane; Satyajit Patel; Ganesh Rathod**

https://hdl.handle.net/10539/45494
WOS

Downloaded from a DSpace repository. https://dspace.org/

# Characterization and Performance Evaluation of Angular-Shaped Fly Ash Aggregates for Pavement Base and Subbase Applications

Hrishikesh A. Shahane, Ph.D.[1]; Satyajit Patel, Ph.D.[2]; and Ganesh W. Rathod, Ph.D.[3]

Downloaded from ascelibrary.org by Univ of Witwatersrand on 04/09/25. Copyright ASCE. For personal use only; all rights reserved.

**Abstract:** This study presents the results of an extensive laboratory investigation on the characterization of angular-shaped fly ash aggregates (FAAs) and their potential as an innovative alternative to natural stone aggregates for pavement materials. The FAAs were produced by curing fly ash blocks in hot water and crushing them into the required sizes of coarse aggregates. The characteristics of the FAAs were correlated with the specifications of the Indian Road Congress. The experimental program comprised experiments such as particle size analysis, heavy Proctor compaction, California bearing ratio (CBR), and repeated load triaxial tests. The performance of two distinct types of FAA in the pavement base and subbase layers was assessed using repeated load triaxial tests at various stress levels. The CBR test results met the criteria for base and subbase layer materials. The resilient modulus ($M_r$) values of FAA ranged from 105 to 180 MPa, which reveals its practicality compared to natural stone aggregates. Additionally, the fit of various existing models for the observed resilient modulus and permanent strain data was examined, and the model parameters for FAA in the best-fitting model were identified. Finite-element analysis indicated that the pavement's service life using FAA as the base material was approximately 15% longer than that of a pavement with a natural aggregate (NA) base layer. Results also demonstrate that the FAA would perform satisfactorily and fulfill the requirement of pavement material. The angular shape and rough surfaces of the proposed FAA are beneficial for better interlocking and result in higher frictional capabilities and low permanent deformation. A comprehensive cost analysis indicates that using FAA for constructing flexible road pavement reduces material costs by 50% compared to using NA. The use of FAA decreases natural aggregate consumption and encourages the usage of waste material in the construction industry. **DOI: 10.1061/JPEODX.PVENG-1705.** *© 2025 American Society of Civil Engineers.*

**Author keywords:** Fly ash aggregates; California bearing ratio; Cyclic loading; Resilient modulus; Permanent deformation; Finite-element analysis.

## Introduction

With their inherent quality and durability, natural aggregates (NAs) remain among the ideal choices in the construction industry. However, there is a shortage of the required quality of NA due to the reduction of natural deposits and the environmental policy of local government bodies. Renewable construction materials, such as those that partially replace composition through waste, can help retrain the depletion of nonrenewable resources and minimize the utilization of NAs. Doing so reduces our environmental impact, avoids environmental dangers, and promotes sustainable growth (Balarim et al. 2024). This has to deviate attention from extensive usage of NAs to the application of recyclable and secondary aggregates in various construction works as well as for the road subbase and base layer application.

Recycled materials have attracted attention as sustainable replacements for conventional aggregates for pavement construction owing to their commercial and environmental interest. Recycled materials commonly used in pavement constructions are reclaimed concrete aggregates, reclaimed asphalt pavements (RAP), crushed brick, and industrial waste for example slags, fly ash, etc. (Tuladhar et al. 2020; Ambekar and Shahane 2021). Arulrajah et al. (2011) used crushed bricks in the pavement subbase. The experimental results specify that crushed bricks blended with other long-lasting recycled aggregates enhance the performance of the subbase layer of flexible pavement. Puppala et al. (2011) investigated the properties of RAP aggregate for use as flexible pavement construction materials. The investigation shows that RAP could be successfully used in the base layer of road construction. Construction and demolished (C&D) waste may be utilized as an option for conventional aggregates in various civil engineering and pavement construction works (Aatheesan et al. 2010; Li et al. 2023). C&D waste produces a relatively lower permanent strain and higher resilient modulus than that of conventional granular subbase materials (Arulrajah et al. 2013). Shahu et al. (2013) also examined the properties of fly ash–dolime–copper slag mix for its efficient use as the construction material of flexible pavements. For the base course, a dolime (15%) stabilized blend of 20% fly ash + 80% copper slag is proposed. Similarly, fly ash has also been utilized for the construction of roads (Yoon et al. 2009; Pai et al. 2021). Arisha et al. (2017) investigated the possibility of utilizing construction and demolition waste materials, namely, mixes of recycled clay

[1]Postdoctoral Fellow, School of Civil and Environmental Engineering, Faculty of Engineering and Built Environment, Univ. of the Witwatersrand, Johannesburg WITS 2050, South Africa (corresponding author). ORCID: https://orcid.org/0000-0003-3339-2234. Email: shahane.hrishi@gmail.com

[2]Associate Professor, Dept. of Civil Engineering, S. V. National Institute of Technology, Surat, Gujarat 395007, India. Email: spatel@amd.svnit.ac.in

[3]Senior Lecturer, School of Civil and Environmental Engineering, Faculty of Engineering and Built Environment, Univ. of the Witwatersrand, Johannesburg WITS 2050, South Africa. ORCID: https://orcid.org/0000-0002-0219-107X. Email: ganesh.rathod@wits.ac.za

Note. This manuscript was submitted on July 9, 2024; approved on February 18, 2025; published online on April 4, 2025. Discussion period open until September 4, 2025; separate discussions must be submitted for individual papers. This paper is part of the ***Journal of Transportation Engineering, Part B: Pavements***, © ASCE, ISSN 2573-5438.

masonry and recycled concrete aggregate, as an unbound granular blend for the construction of roads. The study indicates that the performance of the base and subbase layers constructed with recycled materials was comparable to those constructed with virgin aggregates.

On the other hand, coal available in India is of low grade and produces a huge quantity of ash in the range of 30%–45% (CEA 2020). Therefore, a wide area of valuable land is required for its dumping. In the years 2019 and 2020, the cement sector utilized the maximum amount of fly ash, followed by reclamation of the low-lying area, the raising of ash dyke, bricks and tiles manufacturing, roads and flyover construction, mine filling, etc. Still, about 17% of fly ash remained unutilized (CEA 2020). Production of artificial aggregates with fly ash is one of the potential options for consuming fly ash in huge quantities. Fly ash aggregates (FAAs) can find promising applications in road and embankment construction by replacing natural stone aggregates and gravel [B. Nayak, "A process for manufacture of cold bonded aggregate pellet from fly ash of thermal power plant for constructional use," Indian Patent No. 216945 (2001)]. Mondem and Balunaini (2024) recently manufactured artificial aggregates for pavement applications using mine overburden waste from the coal mining industry and fly ash from thermal power plants. A study demonstrates the satisfactory performance of artificial aggregates against impact and abrasion loading. Similarly, Singh and Patel (2024) reported that artificial fly ash aggregate's (AFA's) impact, crushing, abrasion, and soundness values are well within the allowable limits recommended by the Indian Road Congress for the granular base layer of pavement. Natural aggregates can be replaced fully or partially with the fly ash aggregates in the WMM layer, and AFA may demonstrate good performance under traffic loading. Besides, the angular-shaped (having wear edges and corners) FAA produced by Shahane and Patel (2021, 2022) is reasonably strong, tough, hard, and durable, which additionally satisfies the desired specifications for road aggregates. Numerous investigators (Hicks and Monismith 1971; Allen and Thompson 1974; Thom and Brown 1989; Barksdale and Itani 1989) have described that crushed aggregate with angular to subangular-shaped granules has greater load-distributing capabilities than uncrushed gravel having subrounded or round granules.

To date, the pelletization process and sintering method of hardening have been used largely for manufacturing the FAA (Baykal and Döven 2000; Vasugi and Ramamurthy 2014; Lau et al. 2017; Shivaprasad and Das 2018; etc.). The two main disadvantages of the FAA produced with the aforementioned procedures include the pelletization process producing round-shaped aggregates, and hence the loose aggregate packing and insignificant interlocking capabilities, resulting in decreased load-bearing capability. The usage of greater amounts of energy and the costly, time-consuming, and intricate approach to producing aggregates from a mixture of fly ash and other additives have also been observed. As a result, these aggregates are rarely used on a wide basis in civil engineering applications. Also, due to the absence of appropriate technical data and design guidelines, these aggregates are not used on a full scale in civil construction, particularly in pavement applications.

A review of the scientific literature reveals that research has been done on the characterization of recycled materials for their use in pavement. Nonetheless, there is a lack of research on the most beneficial approaches to using FAA as pavement construction materials. Using innovative materials to construct the pavement requires thorough technical, economic, and environmental knowledge. When deciding to substitute conventional materials with innovative materials, their engineering properties should be investigated to determine whether or not a material is adequate for utilization. Evaluation of engineering properties, permanent deformation characteristics, and the resilient response of angular-shaped FAA is a crucial part of the procedure to implement FAA in pavement base and subbase construction.

The data provided in this paper are significant as, currently, few studies are present in the literature that have examined the engineering properties and behavior of FAA under cyclic loading for pavement application. Therefore, the main objective of this study is to investigate the permanent strain behavior and the resilient response of angular-shaped FAA for their actual application in the construction of flexible pavements. Additionally, finite-element analysis is likewise accomplished to assess the effectiveness of a normal flexible pavement with a base course constructed of FAA.

## Raw Materials and Experimental Program

Fly ashes were obtained from Reliance Industries, Ltd., and Gujarat Industries Power Company, Ltd., Surat, India, separately. Based on the chemical compositions (Table 1), Fly Ash-1 and Fly Ash-2 are classified as 'Class F' and 'Class C', respectively (ASTM 2017). Hydrated lime is used as an additive throughout the work. A heavy compaction test was conducted on the fly ash–lime mix as per IS 2720-Part VIII (IS 2015). Maximum dry unit weights of 11.30 and 13.44 $kN/m^3$ were found at the optimum moisture content of 26% and 29.5% for 96% Class F fly ash + 4% lime (96F1 + 4L) mix and 98% Class C fly ash + 2% lime (98F2 + 2L) mix, respectively.

### *Production of Fly Ash Aggregate and Its Characteristics*

The FAA used in this work has been produced as described in other associated papers by Shahane and Patel (2021, 2022). These aggregates are produced by mechanical compaction of fly ash–lime mixture with an appropriate percentage of their maximum dry unit weight and with a suitable percentage of moisture to make rectangular blocks. Then it is followed by hot water curing and crushing of the blocks to the specified gradation of aggregates. FAA is prepared with two different fly ashes and termed Fly Ash Aggregate 1 (FAA 1) and Fly Ash Aggregate 2 (FAA 2). Fig. 1 shows the photograph of FAA 2 used in this study.

### *Gradation of Aggregates*

The Indian Road Congress (IRC 2013), has specified grading for wet mix macadam (WMM) as a base layer and granular subbase

**Table 1.** Chemical and physical properties of raw materials

| Parameters | Color | Specific gravity | $SiO_2$ (%) | $Al_2O_3$ (%) | $Fe_2O_3$ (%) | $SO_3$ (%) | MgO (%) | CaO (%) | $Na_2O$ (%) |
|---|---|---|---|---|---|---|---|---|---|
| Fly Ash 1 | Gray | 1.28 | 44.45 | 25.30 | 5.92 | 4.49 | 0.598 | 10.64 | 0.57 |
| Fly Ash 2 | Light brown | 1.64 | 36.80 | 3.82 | 14.78 | 10.03 | 0.895 | 22.40 | 0.55 |
| Lime | White | 2.42 | NT | NT | NT | NT | NT | 63.33 | NT |

Note: NT = not tested.



J. Transp. Eng., Part B: Pavements, 2025, 151(2): 04025024

Downloaded from ascelibrary.org by Univ of Witwatersrand on 04/09/25. Copyright ASCE. For personal use only; all rights reserved.



(a)

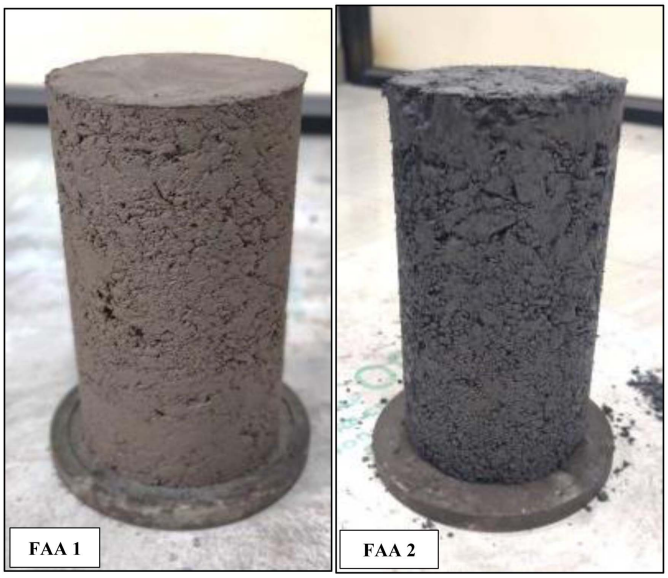


(b)

**Fig. 1.** (a) Fly ash aggregate; and (b) fly ash aggregate specimens. (Images by Hrishikesh A. Shahane.)

(GSB) material having aggregates up to 53 mm in size (Grading V). The gradation of aggregate used in this study for determining the California bearing ratio (CBR) value and $M_r$ value conforms to the Indian Road Congress (IRC) specifications. However, the maximum size of aggregate in the current work was chosen as 20 mm to satisfy the relationship between laboratory mold diameter and maximum particle size, which should be at least 5, especially for triaxial samples as recommended by ASTM standards.

The grading for 20 mm maximum particle size was obtained using the parallel curve technique as shown in Fig. 2. The Talbot's equation in the form shown subsequently can represent the grain size distribution of graded material

$$P = 100\left(\frac{d}{D}\right)^n \tag{1}$$

where $P$ = percentage passing any sieve by weight; $d$ = size of the sieve; and $D$ = maximum size of aggregate. This equation is designated as Fuller's equation, where maximum density generally occurs when the exponent ($n$) equals 0.45 (Sinha 2009).

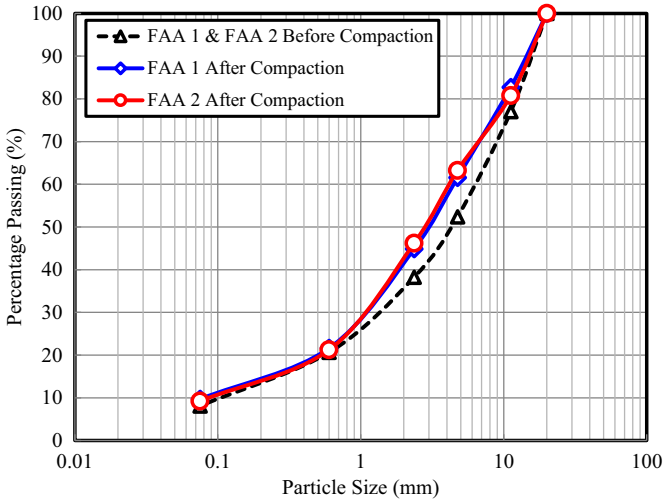


| Coefficient | For Gradation | | |
|---|---|---|---|
| | Adopted Before Compaction | After Compaction | |
| | FAA 1 and FAA 2 | FAA 1 | FAA 2 |
| $C_u$ | 64 | 55 | 51.25 |
| $C_c$ | 3.06 | 3.13 | 3.36 |
| Gradation | Well Graded | Well Graded | Well Graded |

**Fig. 2.** Particle size distribution curve of the fly ash aggregates.

### Compaction Tests

Heavy compaction tests were performed confirm to Indian standard IS 2720 Part VIII (IS 2015). The aggregates were compacted in five layers in a 1,000 $cm^3$ capacity mold. For each layer, 25 nos of blows were given with a 4.9 kg hammer dropped from 450 mm in height. The FAA may be susceptible to crushing during compaction. Therefore, for different moisture content, separate air-dried aggregate samples passing through a 19 mm IS sieve were used. It is vital to note that the water must be fully and appropriately mixed with the FAA because insufficient mixing results in variable test findings. As water absorption of aggregates is high (Table 2), it may be difficult to distribute the water uniformly through the air-dried sample by mixing alone. Consequently, the coarse aggregates were kept for saturation before the testing, and the mixed aggregate sample was stored in a watertight container for 12 h before conducting the test.

### California Bearing Ratio Test

The CBR test was performed on WMM as well as GSB grading aggregate samples as per IS 2720 Part XVI (IS 2018). The aggregates used for the tests were passed through a 20 mm IS sieve. Dynamic compaction was done by taking a representative sample of the aggregates, mixing them uniformly with the optimum quantity of water, and compacting them to the maximum dry unit weight determined as per IS 2720 Part VIII (IS 2015) on selective aggregate gradation. After preparation, the samples were soaked in water for 96 h before testing.

### Repeated Load Triaxial Test

To measure the permanent strain and resilient modulus, repeated load triaxial (RLT) tests were executed. Due to a typical variance of $M_r$ value, three identical specimens were examined for each aggregate. A haversine-shaped wave load pulse was used to replicate traffic wheel loading. A loading period and a resting period were selected as 0.1 and 0.9 s, respectively, and stress levels were selected as per the AASHTO T 307 (AASHTO 2000) recommendation.

Downloaded from ascelibrary.org by Univ of Witwatersrand on 04/09/25. Copyright ASCE. For personal use only; all rights reserved.

**Table 2.** Physical and mechanical properties of aggregates

| Parameters | Authors' results | | | MoRTH-2013 requirements (IRC 2013) |
|---|---|---|---|---|
| | FAA 1 | FAA 2 | NA | |
| Specific gravity | 1.30 | 1.74 | 2.65 | — |
| Angularity number | 7 | 7 | 8 | — |
| Dry loose bulk density (kg/m$^3$) | 710 | 890 | 1,534 | — |
| Water absorption (%) | 26 | 24 | 1.5 | — |
| Wet impact value (%) | 21 | 19.3 | 16 | ≤40% subbase ≤30% base courses |
| Crushing value (%) | 28 | 23 | 19.1 | — |
| Los Angeles abrasion value (%) | 35 | 36 | 20.2 | ≤40% for base courses |
| Soundness in $Na_2SO_4$ (%) (five cycles) | 10 | 9 | 4.6 | ≤12% |
| CBR (%) for WMM grading | 111 | 116 | 100 | — |
| CBR (%) for GSB grading | 90 | 105 | 80 | ≥30% |

During the conditioning phase, 10,000 cycles were initially applied to specimens. The permanent strain is calculated in this phase using the accumulated axial deformation measured throughout the loading cycle. The resilient moduli were determined after the conditioning phase by relating 15 different stress levels.

RLT tests were executed on FAA and NA with 100 mm × 200 mm specimens having a maximum particle size of 20 mm in WMM. These specimens were prepared in a split mold. The 20 mm size aggregates obtained using the parallel curve technique were oven-dried prior to the sample preparation for 24 h at 105°C. Then, the required quantity of aggregates was mixed with the optimum quantity of water as determined from the modified compaction test. This mix was kept in a sealed container for 12 h to make moisture uniformity through the sample and then compacted in the split mold to achieve the required dry unit weight determined from the compaction test. Fig. 1 displays the photograph of the fly ash aggregate specimens.

## Results and Discussion

### Engineering Properties

A photograph of FAA 2 used in this study is shown in Fig. 1(a). These aggregates have an angular shape and rough surfaces. These physical characteristics of the proposed aggregates are beneficial for better interlocking and result in higher frictional capabilities. Table 2 shows the physical and mechanical characteristics of the produced FAA. These characteristics are compared with the specifications of the road laid by the Indian Road Congress (IRC 2013). FAA has about 40% lower specific gravity than NA, and it strongly depends on the specific gravity of the source fly ash and the chemical compounds that form during the pozzolanic reaction among fly ash and additives. The angularity numbers of 7 and 8 were obtained for FAA and NA individually. Singh and Patel (2024) also reported angularity numbers in the range of 7–8 for different types of fly ash aggregates. The results of bulk density and angularity number show that the weight, shapes, and sizes of FAA are similar to those of NA.

Consequently, the lower value of dry, loose bulk density is noted for both aggregates. Water absorptions in FAA were significantly higher than those of NA owing to lower particle density and higher porosity. Furthermore, results confirmed that even though the water absorption value of the aggregates is high, in wet conditions also, the proposed aggregates show superior performance under the impact loading condition. Los Angeles abrasion and soundness values of FAA were found to be within the allowable limits suggested by IRC for pavement granular layers. The results show that the proposed aggregates are adequately tough, hard, strong, and durable. The Los Angeles abrasion value is high, and, therefore, proposed aggregates are not recommended for the wearing course of the pavement.

### Compaction Characteristics

As the resilient performance of granular materials is influenced by density and moisture content (Lekarp et al. 2000), it is crucial to evaluate the precise optimum moisture content and maximum dry unit weight of FAA. The gradation curve of FAA before and after compaction for WMM grading is given in Fig. 2. The results demonstrated that unavoidable breakdowns occurred during compaction. However, the gradations of FAA are not much changed due to compaction and remain well-graded even after the compaction, and this will likely benefit the procedure of compaction. Similar results were obtained for GSB grading (not shown here).

The compaction curves of FAA are given in Fig. 3 with the zero-air-void (ZAV) line. Maximum dry unit weights of 11.20 and 14.10 kN/m$^3$ were found at OMC of 29.6% and 26.9% for well-graded FAA 1 and FAA 2, respectively. The maximum dry unit weight value was obtained higher for FAA 2 aggregates than for FAA 1 aggregates. This is because of the higher specific gravity of FAA 2 aggregates than that of FAA 1 aggregates. Alternatively, the OMC was found to be higher for FAA 1 aggregates and lower for

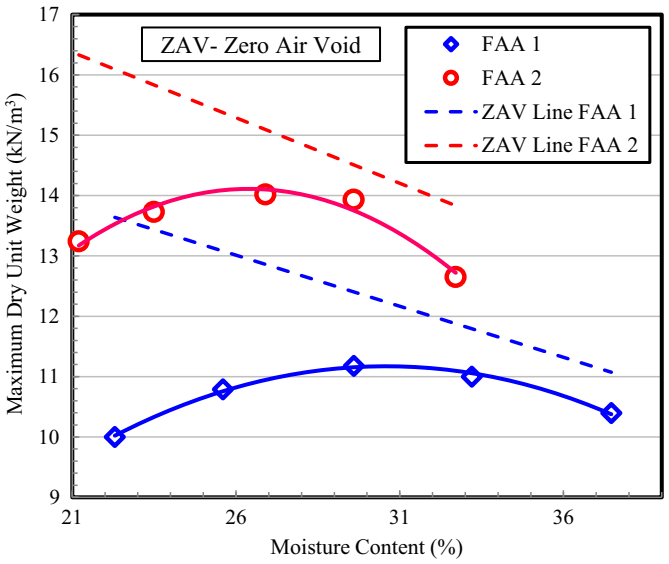


**Fig. 3.** Variation of maximum dry unit weight with moisture content for fly ash aggregates.



J. Transp. Eng., Part B: Pavements, 2025, 151(2): 04025024

Downloaded from ascelibrary.org by Univ of Witwatersrand on 04/09/25. Copyright ASCE. For personal use only; all rights reserved.

FAA 2 aggregates. The discrepancy in OMC is primarily due to differences in aggregate water absorption (Table 2). The OMC values are approximately 3% higher than the water absorption of both aggregates separately, which suggests that the individual percentage of water required for lubrication during the compaction is almost the same for both FAAs.

### California Bearing Ratio

The CBR values of fly ash aggregates were reported as 111% and 116% for FAA 1 and FAA 2 aggregates, independently (Table 2), concerning WMM grading and satisfying the requirement of CBR value for a base and subbase material (IRC 2013). Similarly, both FAA fulfill the requirement for a minimum CBR value of 30% for the subbase layer with GSB grading (IRC 2013). The CBR values of WMM grading are higher than those of GSB grading due to the well-graded aggregates of WMM materials and the presence of more nonplastic fine particles with the respective open-graded aggregates of GSB material. With their wear of edges and corners, angular-shaped fly ash aggregates are perfectly interlocked with each other, resulting in a CBR value comparable to natural stone aggregates.

### Resilient Modulus

The integrating influence of cyclic deviator stress and confining pressure on the resilient modulus ($M_r$) of the FAA 1 is shown in Fig. 4. When deviator stress is increased or confining pressure is applied, the resilience modulus increases. At 93.1 kPa of deviator stress, the $M_r$ value of the FAA 1 increases by 13% when the confining pressure is increased from 34.5 to 137.9 kPa. Similarly, at 34.5 kPa of confining pressure, the $M_r$ values of the FAA 1 aggregates increase by 17% when deviator stress is increased from 31.0 to 93.1 kPa. For FAA 2 aggregate, comparable observations trends and curves (not presented here) of $M_r$ values were found. As confinement increases, the lateral strain in the specimen decreases, resulting in less axial deformation and, consequently, higher stiffness and $M_r$ value.

The $M_r$ value increases with the increase in deviator stress. This phenomenon is the strengthening of a soil sample due to the relocation of soil particles that occurs within the sample due to load repetitions so that the soil hardens and strengthens. As the dislocation density increases, the further deformation of the material becomes difficult. This phenomenon is known as strain hardening. Arulrajah et al. (2011, 2012, 2013) reported that strain hardening takes place in unbound aggregates. In the present case, FAAs are interlocked with each other owing to their angular shape, and the deviator stresses applied are considerably lower compared to the compressive strength of the FAA; as a result, strain hardening occurs. Numerous investigators (Hicks and Monismith 1971; Allen and Thompson 1974; Thom and Brown 1989; Barksdale and Itani 1989) have described that crushed aggregate with angular-shaped granules has greater load-distributing capabilities than uncrushed gravel having round granules, and comparable results were found in this investigation. A rough surface of particles is additionally expected to produce a greater resilient modulus. Barksdale and Itani (1989) tested different aggregates and reported that the resilience modulus of rough, angular crushed aggregates was considerably greater than that of round gravel.

Fig. 4 explains that, as confining pressure increases, the percentage of increase in resilient modulus with deviator stress reduces. This specifies that, at higher confining stresses, deviator stress has a lesser effect on the resilient modulus. The specimen becomes stiffer when confinement increases at any given deviator stress, which results in lower permanent deformation. Puppala et al. (2011) described comparable behavior of base materials.

The base and subbase layers are prone to experiencing 34.5 kPa confining pressure and 103.5 kPa deviator stress under standard pavement design (NCHRP 2003). As a result, the stress pair in Table 2 of AASHTO T307 (AASHTO 2000) at Sequence 6 is nearer to these values and taken as reference stresses for assessment of the $M_r$ value of FAA. Both FAAs show higher $M_r$ values than natural WMM aggregates at 34.5 kPa cell pressure (Fig. 5). Results show that the $M_r$ values of the FAAs were around 10% to 25% higher compared to those of natural WMM aggregates. This indicates that using FAA in place of WMM and GSB can reduce the thickness of the base and subbase, separately. Consequently, if NA is substituted partially or fully with FAA in the WMM layer, FAA may demonstrate good performance under traffic loading.

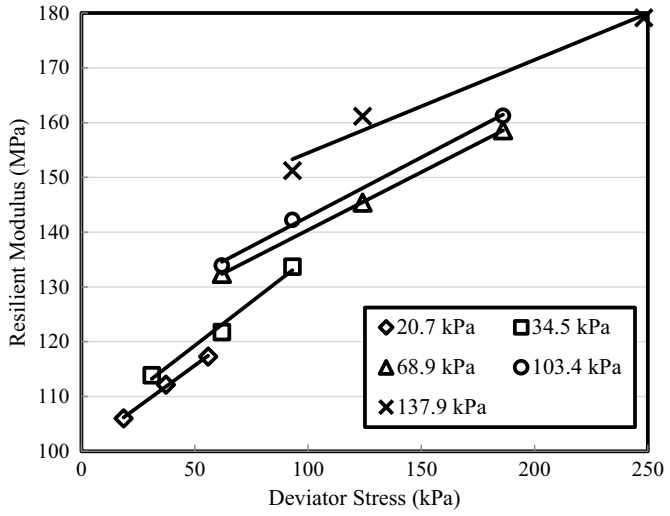


**Fig. 4.** Influence of deviatoric and confining stresses on resilient modulus of FAA 1.

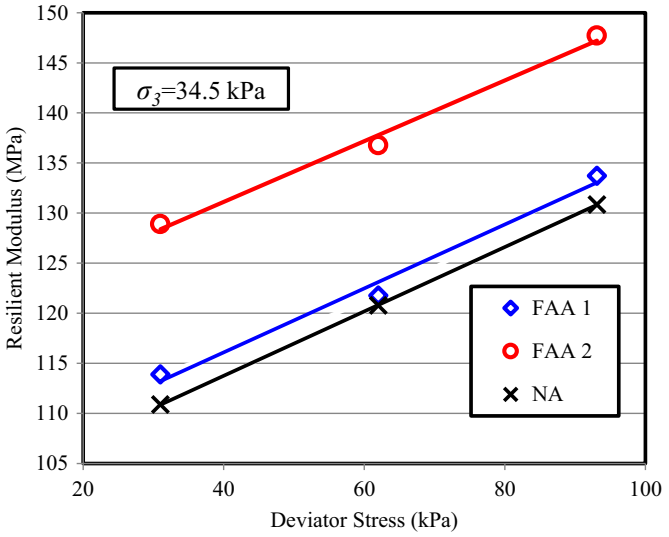


**Fig. 5.** Resilient modulus versus deviator stress relationship for fly ash aggregates and natural aggregates (WMM Grading) at a constant cell pressure of 34.5 kPa.

Downloaded from ascelibrary.org by Univ of Witwatersrand on 04/09/25. Copyright ASCE. For personal use only; all rights reserved.

### Modeling of Resilient Modulus Response

The resilient modulus ($M_r$) can be predicted by using constitutive models at different deviator stresses and cell pressures. The outcomes of the five models are compared according to the following constraints:

1. Model 1: The two-parameter $k$-$\theta$ model suggested by Hicks and Monismith (1971)

$$M_r = k_1 \cdot \theta^{k_2} \tag{2}$$

2. Model 2: The two-parameter model recommended by Witczak and Uzan (1988)

$$M_r = k_3 \cdot \sigma_d^{k_4} \tag{3}$$

3. Model 3: The three-parameter NCHRP model proposed by NCHRP (1997) and Puppala et al. (2011)

$$\frac{M_r}{P_a} = k_5 \left(\frac{\sigma_3}{P_a}\right)^{k_6} \cdot \left(\frac{\sigma_d}{P_a}\right)^{k_7} \tag{4}$$

4. Model 4: The three-parameter model proposed by Uzan (1985)

$$\frac{M_r}{P_a} = k_8 \left(\frac{\theta}{P_a}\right)^{k_9} \cdot \left(\frac{\sigma_d}{P_a}\right)^{k_{10}} \tag{5}$$

5. Model 5: The three-parameter octahedral shear stress model used in the Mechanistic-Empirical Pavement Design Guide AASHTO (2008) is as follows:

$$\frac{M_r}{P_a} = k_{11} \left(\frac{\theta}{P_a}\right)^{k_{12}} \cdot \left(\frac{\tau_{oct}}{P_a} + 1\right)^{k_{13}} \tag{6}$$

where $\theta$ (bulk stress) = $\sigma_d + 3\sigma_3$; $\sigma_3$ = confining stress; $\sigma_d$ = cyclic deviatoric stress; $P_a$ = atmospheric pressure (=100 kPa); $\tau_{oct}$ (octahedral shear stress) = $1/3\{(\sigma_1-\sigma_2)^2 + (\sigma_1-\sigma_3)^2 + (\sigma_2-\sigma_3)^2\}^{0.5}$; and $k_1$ to $k_{13}$ = model constants.

Regression analysis of measured data was carried out, and model constants $k_1$ to $k_{13}$ were determined. $M_r$ values were back-calculated for different aggregates using these model constants at all 15 stress levels [Table 2 of AASHTO T307 (AASHTO 2000)]. The coefficient of determination ($R^2$) and residual sum of squares (RSS) for all five models were calculated by comparing predicted and measured $M_r$ values, as shown in Table 3. Model 5 had the highest $R^2$ value and the lowest RSS value, showing that the three-parameter octahedral shear stress model predicts the best resilient modulus for fly ash aggregates.

The relationship between the measured and predicted $M_r$ values of the octahedral shear stress model is presented in Fig. 6. Table 4 shows the model constants calculated for various aggregates. Higher values of $k_{11}$ specify that deviator stress has a greater effect on $M_r$ values than that of confining pressure. Positive $k_{13}$ values show that stress hardening occurs in fly ash aggregates; i.e., at constant cell pressure, with the increase in deviator stress $M_r$ values also increases. Puppala et al. (2011) described the comparable performance of cement-treated aggregates.

**Table 3.** $R^2$ and RSS for various stress-dependent models for fly ash aggregates

| Stress-dependent model | $R^2$ | RSS |
|---|---|---|
| $M_r = k_1 \cdot \theta^{k_2}$ | 0.91 | 1,222 |
| $M_r = k_3 \sigma_d^{k_4}$ | 0.91 | 593 |
| $\frac{M_r}{P_a} = k_5 \cdot \left(\frac{\sigma_3}{P_a}\right)^{k_6} \cdot \left(\frac{\sigma_d}{P_a}\right)^{k_7}$ | 0.98 | 296 |
| $\frac{M_r}{P_a} = k_8 \cdot \left(\frac{\theta}{P_a}\right)^{k_9} \cdot \left(\frac{\sigma_d}{P_a}\right)^{k_{10}}$ | 0.98 | 307 |
| $\frac{M_r}{P_a} = k_{11} \cdot \left(\frac{\theta}{P_a}\right)^{k_{12}} \cdot \left(\frac{\tau_{oct}}{P_a} + 1\right)^{k_{13}}$ | 0.99 | 167 |

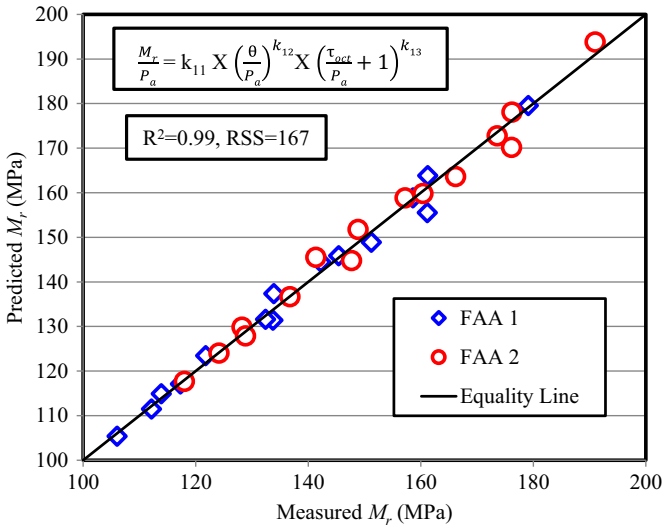


**Fig. 6.** Measured resilient modulus versus predicted resilient modulus using Model 5 for fly ash aggregates.

### Permanent Strain Characteristics

Rutting in flexible pavement occurs mainly due to the high plastic strain developed in the subgrade layer. Consequently, to use FAA in flexible pavements, it is crucial to thoroughly analyze their permanent strain behavior. Permanent deformation is an important parameter to consider in the design process (Venkatesh et al. 2020).

A plot depicting permanent strain values versus loading cycles, shown in Fig. 7, is generated at a constant cell pressure to quantify the permanent strain behavior of aggregates. For all types of aggregates, the permanent strain initially increases rapidly with the number of load cycles and then shows a constant value after 5,000 cycles. FAA shows a smaller maximum permanent strain value than the WMM aggregates after 10,000 load cycles. These findings are opposite to the resilient modulus. Patel and Shahu (2016) also specified that the lower maximum permanent strain will occur with a higher resilient modulus.

These results indicate that angular-shaped (having wear edges and corners) FAAs recommended in this study, having characteristics similar to those of NAs, can perform about the same in terms of permanent deformation due to their shape. In addition, angular aggregates have a higher solid volume; therefore, particle packing is denser. Barksdale and Itani (1989) reported that crushed cubic aggregates were less responsive to rutting than rounded gravel with smooth surfaces and rounded corners.

**Table 4.** Model constants for different aggregates

| | $\frac{M_r}{P_a} = k_{11} \cdot \left(\frac{\theta}{P_a}\right)^{k_{12}} \cdot \left(\frac{\tau_{oct}}{P_a} + 1\right)^{k_{13}}$ | | | $\varepsilon_p = a + b \log_e (N)$ | |
|---|---|---|---|---|---|
| Material | $k_{11}$ | $k_{12}$ | $k_{13}$ | $a$ | $b$ |
| NA | 0.864 | 0.138 | 0.491 | 838.9 | 161.28 |
| FAA 1 | 1.051 | 0.132 | 0.370 | 588.78 | 159.48 |
| FAA 2 | 1.175 | 0.129 | 0.329 | 556.29 | 160.51 |

Downloaded from ascelibrary.org by Univ of Witwatersrand on 04/09/25. Copyright ASCE. For personal use only; all rights reserved.

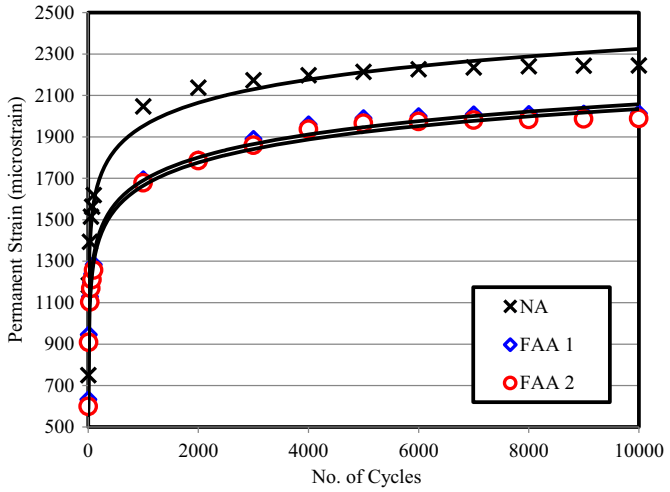


**Fig. 7.** Variation of permanent strain with loading cycles for different aggregates.

### Permanent Strain Modeling

1. Model 1: The logarithmic model proposed by Barksdale (1972) and Bennert et al. (2000)

$$\varepsilon_p = a + b\log_e(N) \tag{7}$$

2. Model 2: A two-parameter power model suggested by Peerapong and Hamid (2009)

$$\varepsilon_p = cN^d \tag{8}$$

where $\varepsilon_p$ = permanent strain; $a$, $b$, $c$, and $d$ = model constants; and $N$ = number of load repetitions.

Table 4 shows the values of model constants for different aggregates obtained by regression analysis for the logarithmic model. The logarithmic model offers the best prediction of permanent strain for FAA with its maximum $R^2$ value and minimum RSS. The relationship between predicted $\varepsilon_p$ values and measured $\varepsilon_p$ values for the FAA is presented in Fig. 8 with an excellent $R^2$ value of 0.99 and a lower RSS of 40,687. This shows how the logarithmic model could be applied to predict the development of permanent strain in FAA.

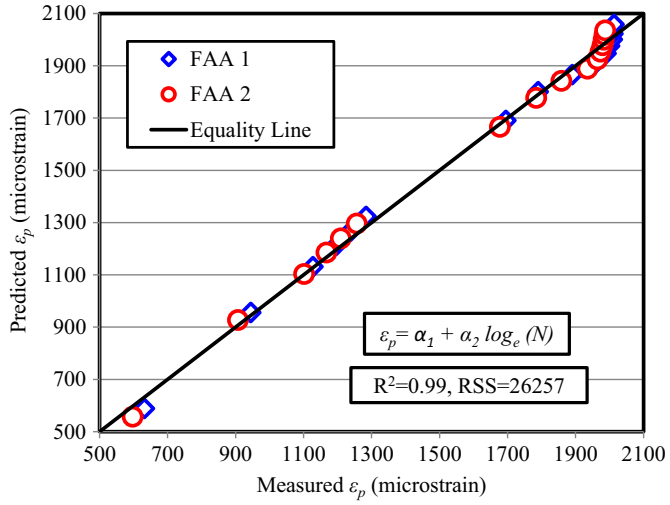


**Fig. 8.** Measured plastic strain versus predicted plastic strain using logarithmic model for fly ash aggregates.

### Service Life of Pavements

To determine the construction and maintenance cost of the pavement, pavement service life is an important factor. A commercial finite-element program, Plaxis 3D, is used to perform a finite-element analysis of five-layered flexible pavement systems. In the various regions of India, subgrade soil is often expansive soil, with soaked CBR values of 3% to 4%. A typical flexible pavement with thicknesses of various layers for traffic intensity of 100 million standard axles (MSA) using subgrade CBR of 3% and 4%, respectively, as determined by IRC 37 (IRC 2018), is shown in Fig. 9. The figure also shows the meshing of the finite elements and the boundary dimensions used in this work after a short parametric study on the convergence of results. For the analysis of the dense bituminous macadam (DBM) and bituminous concrete (BC) layer, a linear-elastic model is used, and for the subgrade, subbase, and base layers, a Mohr–Coulomb model is used. Table 5 presents the input parameters used in the analysis corresponding to different layers. The $M_r$ values were evaluated by experimentation for natural WMM aggregates, FAA, and GSB material conforming to 34.5 and 93.1 kPa of confining pressure and cyclic-deviator stress, respectively.

As per IRC 37 (IRC 2018), the following equations are used to determine the service life ratio (SLR) of flexible pavements:

$$(\text{SLR})_{\text{fatigue}} = (\varepsilon_{t1}/\varepsilon_{t2})^{3.89} \tag{9}$$

$$(\text{SLR})_{\text{rutting}} = (\varepsilon_{v1}/\varepsilon_{v2})^{4.5337} \tag{10}$$

where $\varepsilon_{t1}$ and $\varepsilon_{t2}$ = maximum horizontal tensile strains developed at the bottom of the DBM layer; and $\varepsilon_{v1}$ and $\varepsilon_{v2}$ = maximum vertical compressive strains developed at the top of subgrade soil prepared with NA and that of FAA as WMM, separately. Table 6 shows the $\delta$, $\varepsilon_{t1}$, $\varepsilon_{t2}$, $\varepsilon_{v1}$, $\varepsilon_{v2}$, and SLR values. By using FAA in a base course material, around 15% greater service life can be achieved. Similarly, pavement surface deformation is reduced correlated to the natural WMM layer.

Furthermore, the layer coefficient $a_2$ for base courses constructed with FAA can be determined by applying the equation provided by AASHTO (1993)

$$a_2 = 0.249(\log M_r) - 0.977 \tag{11}$$

where $M_r$ = resilient modulus of the base layer in psi. The average $M_r$ values for WMM, FAA 1, and FAA 2 bases were ascertained by experimentation. The variation of the base layer coefficient of fly ash aggregates and conventional aggregate determined by the AASHTO method is given in Fig. 10. The coefficients of the base layer for WWM materials ranged from 0.05 to 0.10, while FAA showed coefficients ranging from 0.07 to 0.12. These results demonstrate that the FAA behaves similarly to NA.

### Cost Analysis

A detailed cost analysis of the FAA has been conducted for setting up a pilot plant of capacity 40 t per day. The various parameters considered are the capital required; raw material cost; electricity expenses; manpower requirement; depreciation of buildings, plants, and machinery; total maintenance cost, etc. For economical manufacture, FAA can be cured using hot water from thermal power plant cooling towers. The cost of fly ash is also excluded, with the assumption that the pilot plant will be installed in the

Downloaded from ascelibrary.org by Univ of Witwatersrand on 04/09/25. Copyright ASCE. For personal use only; all rights reserved.

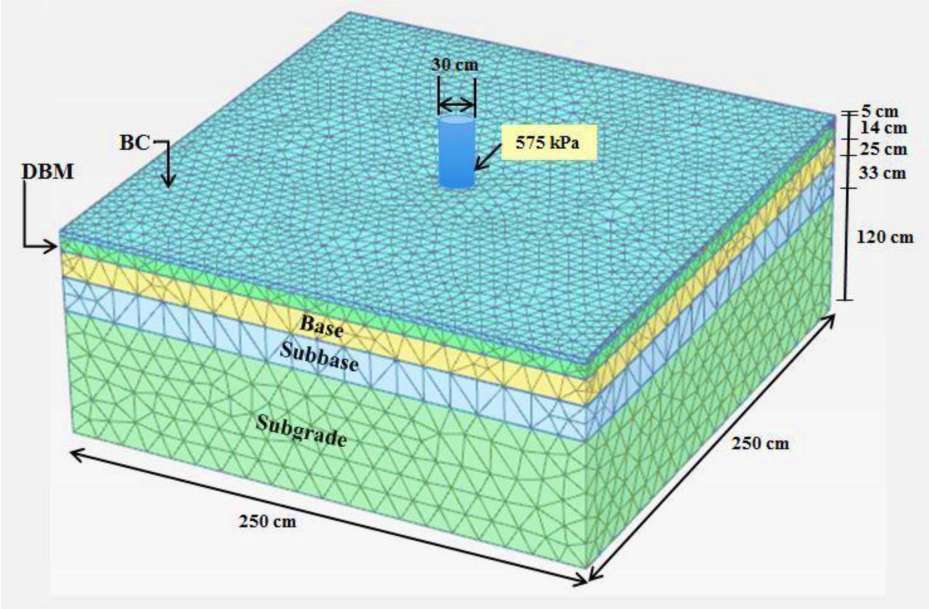


**Fig. 9.** Finite-element analysis of flexible pavement system using Plaxis for traffic intensity of 100 msa and subgrade CBR of 4%.

**Table 5.** Parameters used for the finite-element analysis of pavement system

| Parameter | 3% CBR subgrade | 4% CBR subgrade | Subbase (GSB) | Base course | | | DBM | BC |
|---|---|---|---|---|---|---|---|---|
| | | | | NA[a] | FAA 1[a] | FAA 2[a] | | |
| $M_r$ (MPa) | 30[b] | 40[b] | 100 | 127 | 134 | 148 | 2,000[b] | 2,000[b] |
| $\nu$ | 0.35 | 0.35 | 0.35 | 0.35 | 0.35 | 0.35 | 0.35 | 0.35 |
| $\gamma$ (kN/m$^3$) | 17.7 | 17.9 | 21.4 | 21.8 | 11.3 | 14.0 | 22.6 | 23.3 |
| c (kPa) | 0 | 0 | 0 | 0 | 20 | 20 | — | — |
| $\phi$ (degrees) | 28 | 30 | 43 | 48 | 45 | 45 | — | — |
| Thickness (mm) for 4% CBR | 1,200 | 1,200 | 330 | 250 | 250 | 250 | 140 | 50 |

[a]Determined experimentally.
[b]Data from IRC 37 (IRC 2018).

**Table 6.** Service life ratio (SLR) for fly ash aggregate base course

| CBR (%) | Base course | Thickness (mm) | $\delta$ (mm) | Fatigue failure criteria | | Rutting failure criteria | |
|---|---|---|---|---|---|---|---|
| | | | | $\varepsilon_{t1}$ or $\varepsilon_{t2}$ (mm) | SLR | $\varepsilon_{v1}$ or $\varepsilon_{v2}$ (mm) | SLR |
| 3 | NA | 250 | 0.2598 | 0.01201 | 1.000 | 0.005689 | 1.000 |
| 3 | FAA 1 | 250 | 0.2446 | 0.01131 | 1.263 | 0.005450 | 1.215 |
| 3 | FAA 2 | 250 | 0.2412 | 0.01112 | 1.349 | 0.005353 | 1.318 |
| 4 | NA | 250 | 0.2493 | 0.01196 | 1.000 | 0.005211 | 1.000 |
| 4 | FAA 1 | 250 | 0.2438 | 0.01144 | 1.189 | 0.005349 | 1.250 |
| 4 | FAA 2 | 250 | 0.2438 | 0.01145 | 1.185 | 0.005368 | 1.320 |

Note: $\delta$ = maximum deformation at the pavement surface.

vicinity of the thermal power station. Interest-related, administrative, office, marketing, and travel expenses have not been included. Assuming 1% raw material waste, the costs for 4% lime and 27% water are included in the raw material cost. Additionally taken into account is the average national capacity utilization factor, or plant load factor of 95%. Table 7 provides further adopted values for the factors under consideration.

Fig. 11 estimates a total cost of production is USD 6.5/m$^3$. The cost of raw materials (lime and water) was found to be the major component of the total cost. The cost of power and other utilities, manpower, depreciation, and maintenance was estimated as 10.76%, 25.95%, 15.11%, and 5.25%, respectively. The cost analysis shows that to validate the economic feasibility, it is crucial to determine the transportation cost of raw materials from the source to the production plant. When aggregate production plants are close to or within the thermal power plants, and the transportation distance of hydrated lime is less than 350 km from the production plant, such projects can be done at an affordable cost (Shahane and Patel 2024). As per the schedule of the rate of the Central Public Works Department (CPWD), New Delhi, India, the cost per cubic meter of natural aggregate (conventional WMM) ranges from $11 to $16 (INR 900 to 1,300) Meanwhile, the





Downloaded from ascelibrary.org by Univ of Witwatersrand on 04/09/25. Copyright ASCE. For personal use only; all rights reserved.

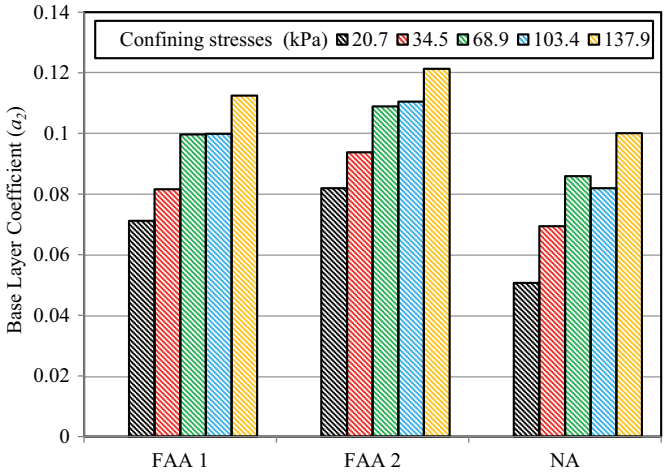


**Fig. 10.** Interpreted base layer structural coefficients of fly ash and natural aggregates.

**Table 7.** Parameters considered for calculating production cost

| Parameter | Values adopted |
|---|---|
| Working days | 300 per year |
| Plant load factor (PLF) | 95% |
| 5% wastage is considered | |
| Brick size | 230 mm × 110 mm × 60 mm |
| Bulk density of brick | 1,500 kg/m$^3$ |
| Bulk density of aggregate | 810 kg/m$^3$ |
| Manpower for 3 shifts | 15 persons |
| Cost of lime | \$47.35/ton |
| Cost of water | \$0.32/ton |
| Cost of electricity | \$0.05/kWh |
| Depreciation cost | 5% for machinery; 2.5% for building |
| Maintenance cost | 3% of cost of plant and machinery |

Note: \$1 = INR 84.

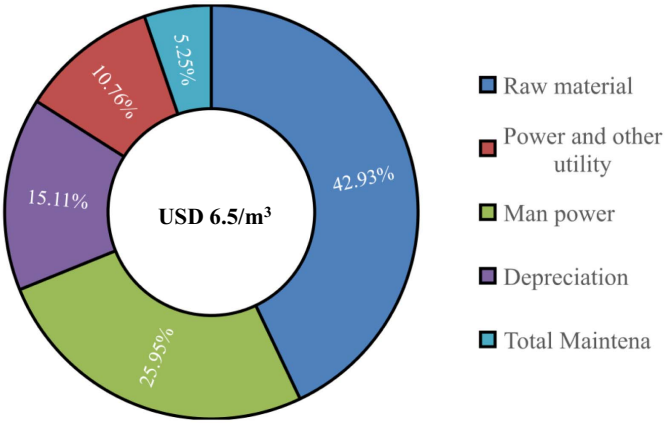


**Fig. 11.** Breakup of production cost for angular-shaped fly ash aggregate determined for plant capacity of 40 tons/day.

manufacturing cost of the proposed FAA is obtained as only \$6 to \$7 (INR 560) per cubic meter. Therefore, by replacing the traditional WMM aggregates with FAA, material costs can be lowered by up to 50%.

**Table 8.** Capital investment for setting up of pilot plant of capacity 40 t/day

| Parameter | Cost in USD |
|---|---|
| Land required (area: 4,500 m$^2$) | Excluded |
| Production shed and installations (area: 600 m$^2$ @ \$118.5 per m$^2$) | 71,100 |
| Plant and machinery | |
| Batching plant (1 No.) | 20,123 |
| Pressing and brick machine (1 No.) | 44,982 |
| Curing instrument | 9,470 |
| Crusher | 33,737 |
| Forklift and loader | 29,002 |
| **Total** | **2,08,414** |

Note: \$1 = INR 84.

The cost of setting up a pilot plant nearby coal-based thermal power stations is also presented in Table 8. It is assumed that the thermal power stations will provide the required land at no cost. The total cost of the shed area was calculated from the item-based rates given in the schedule of rates of CPWD and is included in the pilot plant setup cost. A total cost of \$208,635 (INR 176 lakhs) is estimated for setting up the pilot plant. The cost analysis is based on the standard parameters and may change according to the site location.

## Limitations and Future Work

Several methods for producing and hardening FAA are documented in the literature; however, results are only valid if the produced FAA exhibits similar mechanical and physical characteristics. The water absorption and Los Angeles abrasion values of recommended FAA are higher as correlated to conventional NA; further research may be required to overcome these results. Its susceptibility to freeze–thaw conditions must be evaluated to utilize proposed aggregates in higher altitude areas. In the current investigation, only two types of FAA were used to determine their performance as the base and subbase layer materials. These results may be validated with various types of FAA manufactured with diverse sources of fly ash and prepared with different additives and curing methods. The structural coefficients calculated using the prior methods must still be checked and validated using various methodologies, including field measurements. It is recommended that a small-scale trial section may be constructed with FAA in the field, and its performance should be evaluated under APT axle loading or regular truck traffic before considering a new material as viable.

## Conclusions and Recommendations

This study evaluated two angular-shaped fly ash aggregates for pavement base and subbase applications using RLT testing. The assessment has been performed concerning resilient modulus and permanent deformation properties of angular-shaped FAA according to traffic load circumstances, thereby connecting the gap in understanding the appropriate application of FAA in pavement construction.

- The results reveal that the FAA physical and mechanical characteristics meet the requirements for its usage in the construction of roads. As the Los Angeles abrasion value is higher, proposed aggregates are not recommended for use in the wearing course of the pavement.

Downloaded from ascelibrary.org by Univ of Witwatersrand on 04/09/25. Copyright ASCE. For personal use only; all rights reserved.

- CBR test results of FAA show that proposed aggregates can successfully be utilized as base and subbase layer material in flexible road pavement.
- With an increase in deviator stress, the resilient modulus increases due to the strain-hardening phenomenon. The comparison of Mr values of FAA with that of NA indicates that conventional aggregates can be completely replaced with FAA in the base and subbase layers of flexible pavement without compromising the performance for sustainable road construction.
- The octahedral shear stress model offers the finest fit for FAA. The bulk stress, deviator stress, and confining stress are the governing factors for the FAA resilient modulus.
- The results indicate that angular-shaped (having wear edges and corners) FAA recommended in this study, having characteristics similar to those of NA, can behave comparably to permanent deformation due to their shape. The permanent strain properties of FAA are contradictory to the prevailing trends experimental for Mr values. The higher the resilient modulus, the more resistant to permanent deformation there will be, and the lesser the maximum permanent strain.
- A logarithmic model gives an excellent fit for the assessment of permanent strain development in FAA. It is also evidence that stress level has a greater influence on $\varepsilon$p values than that of load repetitions.
- Finite-element analysis shows that the use of FAA as the base course material has less pavement deformation and about 15% longer service life than natural aggregates. The FAA gives the coefficients of the base layer, ranging from 0.07 to 0.12.
- By using the recommended FAA, the material cost of construction of the flexible pavement can be lowered by up to 50%.

As a result, using FAA in base and subbase courses of pavement provides a double benefit in terms of performance and waste material utilization, which contributes to sustainability. Since this material behaved similarly to NA, it is expected to be used for backfills in walls and embankments in the future.

## Data Availability Statement

Some or all data, models, or code that support the findings of this study are available from the corresponding author upon reasonable request.

## Supplemental Materials

Supplemental Materials associated with this paper are available online in the ASCE Library (www.ascelibrary.org).

## References


AASHTO. 1993. *Guide for design of pavement structures*. Washington, DC: Transportation Research Board.

AASHTO. 2000. *Determining the resilient modulus of soils and aggregate materials*. AASHTO T-307. Washington, DC: AASHTO.

AASHTO. 2008. *Mechanistic-empirical pavement design guide*. Washington, DC: Transportation Research Board.

Aatheesan, T., A. Arulrajah, M. W. Bo, B. Vuong, and J. Wilson. 2010. "Crushed brick blends with crushed rock for pavement systems." In Vol. 63 of *Proc., Institution of Civil Engineers-Waste And Resource Management*, 29–35. Leeds, UK: Emerald Publishing. https://doi.org/10.1680/warm.2010.163.1.29.

Allen, J. J., and M. R. Thompson. 1974. "Resilient response of granular materials subjected to time dependent lateral stresses." In *Proc., 53rd Annual Meeting of the Highway Research Board*, 1–13. Washington, DC: Transportation Research Board.

Ambekar, M. S., and H. A. Shahane. 2021. "Laboratory investigation of black cotton soil-fly ash-steel slag mixes." In Vol. 136 of *Proc., Indian Geotechnical Conf. 2019: IGC-2019 Volume III*, 717–726. Singapore: Springer. https://doi.org/10.1007/978-981-33-6444-8_64.

Arisha, A. M., A. R. Gabr, S. M. El-Badawy, and S. A. Shwally. 2017. "Performance evaluation of construction and demolition waste materials for pavement construction in Egypt." *J. Mater. Civ. Eng.* 30 (2): 1–14. https://doi.org/10.1061/(ASCE)MT.1943-5533.0002127.

Arulrajah, A., Y. M. M. Ali, J. Piratheepan, and M. W. Bo. 2012. "Geotechnical properties of waste excavation rock in pavement subbase applications." *J. Mater. Civ. Eng.* 24 (7): 924–932. https://doi.org/10.1061/(ASCE)MT.1943-5533.0000419.

Arulrajah, A., J. Piratheepan, T. Aatheesan, and M. W. Bo. 2011. "Geotechnical properties of recycled crushed brick in pavement applications." *J. Mater. Civ. Eng.* 23 (10): 1444–1452. https://doi.org/10.1061/(ASCE)MT.1943-5533.0000319.

Arulrajah, A., J. Piratheepan, M. M. Disfani, and M. W. Bo. 2013. "Resilient moduli response of recycled construction and demolition materials in pavement subbase applications." *J. Mater. Civ. Eng.* 25 (12): 1920–1928. https://doi.org/10.1061/(ASCE)MT.1943-5533.0000766.

ASTM. 2017. *Standard specification for coal fly ash and raw or calcined natural pozzolan for use as a mineral admixture in concrete*. ASTM C 618. West Conshohocken, PA: ASTM.

Balarim, N. G., G. Dognani, G. T. A. Santos, S. R. Teixeira, F. S. Okimoto, R. J. D. Santos, F. C. Cabrera, and A. E. Job. 2024. "Eco-friendly construction materials: New gypsum-based composite with dregs waste from the cellulose industry." *Eur. J. Environ. Civ. Eng.* 28 (16): 3875–3893. https://doi.org/10.1080/19648189.2024.2362743.

Barksdale, R. D. 1972. "Laboratory evaluation of rutting in base course materials." In *Proc., 3rd Int. Conf. on Structural Design of Asphalt Pavements*, 161–174. Ann Arbor, MI: Dept. of Civil Engineering, Univ. of Michigan.

Barksdale, R. D., and S. Y. Itani. 1989. "Influence of aggregate shape on base behavior." *Transp. Res. Rec.* 1027: 173–182.

Baykal, G., and A. G. Döven. 2000. "Utilization of fly ash by pelletization process; theory, application areas and research results." *Resour. Conserv. Recycl.* 30 (1): 59–77. https://doi.org/10.1016/S0921-3449(00)00042-2.

Bennert, T., J. Walter, A. Maher, and N. Gucunski. 2000. "Utilization of construction and demolition debris under traffic-type loading in base and subbase applications." *Transp. Res. Rec.* 1714 (1): 33–39. https://doi.org/10.3141/1714-05.

CEA (Central Electricity Authority). 2020. *Report on fly ash generation at coal/lignite based thermal power station and its utilization in the country for the year 2019-20*. New Delhi, India: Central Electricity Authority.

Hicks, R. G., and C. L. Monismith. 1971. "Factors influencing the resilient response of granular materials." *Highway Res. Rec.* 345: 15–31.

IRC (Indian Road Congress). 2013. *Specification for road and bridge works-fifth revision*. New Delhi, India: Ministry of Road Transport and Highway (MoRTH).

IRC (Indian Roads Congress). 2018. *Guidelines for the design of flexible pavements*. IRC 37. New Delhi, India: IRC.

IS (Indian Standard). 2015. *Determination of water content-dry density relation using heavy compaction*. IS 2720 Part-VIII. New Delhi, India: IS.

IS (Indian Standard). 2018. *Laboratory determination of CBR*. IS 2720 Part-XVI. New Delhi, India. IS.

Lau, P. C., D. C. L. Teo, and M. A. Mannan. 2017. "Characteristics of lightweight aggregate produced from lime-treated sewage sludge and palm oil fuel ash." *Constr. Build. Mater.* 152 (Oct): 558–567. https://doi.org/10.1016/j.conbuildmat.2017.07.022.

Lekarp, F., U. Isacsson, and D. A. Andrew. 2000. "State of the art. I: Resilient response of unbound aggregates." *J. Transp. Eng.* 126 (1): 66–75. https://doi.org/10.1061/(ASCE)0733-947X(2000)126:1(66).

Li, L., L. Qin, H. Xiao, Z. Hu, G. Xu, and Q. Ma. 2023. "The triaxial test of construction and demolition (C&D) materials with different particle sizes and sand contents." *Eur. J. Environ. Civ. Eng.* 27 (9): 2800–2821. https://doi.org/10.1080/19648189.2020.1820908.


Downloaded from ascelibrary.org by Univ of Witwatersrand on 04/09/25. Copyright ASCE. For personal use only; all rights reserved.

Mondem, N., and U. Balunaini. 2024. "Manufacturing artificial aggregates from overburden coal mine waste and their properties for pavement applications." *J. Mater. Civ. Eng.* 36 (7): 1–10. https://doi.org/10.1061/JMCEE7.MTENG-17138.

NCHRP (National Cooperative Highway Research Program). 1997. *Laboratory determination of resilient modulus for flexible pavement design*. Washington, DC: Transportation Research Board.

NCHRP (National Cooperative Highway Research Program). 2003. *Harmonized test methods for laboratory determination of resilient modulus for flexible pavement design*. Washington, DC: Transportation Research Board.

Pai, R. R., M. D. Bakare, S. Patel, and J. T. Shahu. 2021. "Structural evaluation of flexible pavement constructed with steel slag–fly ash–lime mix in the base layer." *J. Mater. Civ. Eng.* 33 (6): 04021097. https://doi.org/10.1061/(ASCE)MT.1943-5533.0003711.

Patel, S., and J. T. Shahu. 2016. "Resilient response and permanent strain of steel slag-fly ash-dolime mix." *J. Mater. Civ. Eng.* 28 (10): 04016106. https://doi.org/10.1061/(ASCE)MT.1943-5533.0001619.

Peerapong, J., and N. Hamid. 2009. "Mechanical behaviours of hydrated cement treated crushed rock base as a road base material in Western Australia." *Int. J. Pavement Eng.* 10 (1): 39–47. https://doi.org/10.1080/10298430802342682.

Puppala, A. J., L. R. Hoyos, and A. K. Potturi. 2011. "Resilient moduli response of moderately cement-treated reclaimed asphalt pavement aggregates." *J. Mater. Civ. Eng.* 23 (7): 990–998. https://doi.org/10.1061/(ASCE)MT.1943-5533.0000268.

Shahane, H. A., and S. Patel. 2021. "Influence of curing method on characteristics of environment-friendly angular shaped cold bonded fly ash aggregates." *J. Build. Eng.* 35 (Mar): 101997. https://doi.org/10.1016/j.jobe.2020.101997.

Shahane, H. A., and S. Patel. 2022. "Influence of design parameters on engineering properties of angular shaped fly ash aggregates." *Constr. Build. Mater.* 327 (Apr): 126914. https://doi.org/10.1016/j.conbuildmat.2022.126914.

Shahane, H. A., and S. Patel. 2024. "Comparative environmental life cycle assessment of artificial fly ash aggregates and natural aggregate production in India." *Innovative Infrastruct. Solutions* 9 (3): 69. https://doi.org/10.1007/s41062-024-01382-z.

Shahu, J. T., S. Patel, and A. Senapati. 2013. "Engineering properties of copper slag–fly ash–dolime mix and its utilization in base course of flexible pavements." *J. Mater. Civ. Eng.* 25 (12): 1871–1879. https://doi.org/10.1061/(ASCE)MT.1943-5533.0000756.

Shivaprasad, K. N., and B. B. Das. 2018. "Determination of optimized geopolymerization factors on the properties of pelletized fly ash aggregates." *Constr. Build. Mater.* 163 (Feb): 428–437. https://doi.org/10.1016/j.conbuildmat.2017.12.038.

Singh, S., and S. Patel. 2024. "Characterization and performance evaluation of eco-friendly angular-shaped fly ash aggregates as base material in pavement construction under cyclic and shear loading." *J. Mater. Civ. Eng.* 36 (12): 04024393. https://doi.org/10.1061/JMCEE7.MTENG-18052.

Sinha, A. K. 2009. "Study on subbase materials for rural roads." Accessed August 20, 2021. http://hdl.handle.net/123456789/1662.

Thom, N. H., and S. F. Brown. 1989. "The mechanical properties of unbound aggregates from various sources." In *Unbound aggregates in roads*, edited by R. H. Jones and A. R. Dawson, 130–142. London: Elsevier.

Tuladhar, R., A. Marshall, and N. Sivakugan. 2020. "Use of recycled concrete aggregate for pavement construction." In *Advances in construction and demolition waste recycling*, 181–197. Sawston, UK: Woodhead Publishing.

Uzan, J. 1985. "Characterization of granular materials." *Transp. Res. Rec.* 1022 (1): 52–59.

Vasugi, V., and K. Ramamurthy. 2014. "Identification of admixture for pelletization and strength enhancement of sintered coal pond ash aggregate through statistically designed experiments." *Mater. Des.* 60 (Aug): 563–575. https://doi.org/10.1016/j.matdes.2014.04.023.

Venkatesh, N., M. Heeralal, and R. Pillai. 2020. "Resilient and permanent deformation behaviour of clayey subgrade soil subjected to repeated load triaxial tests." *Eur. J. Environ. Civ. Eng.* 24 (9): 1414–1429. https://doi.org/10.1080/19648189.2018.1472041.

Witczak, M., and J. Uzan. 1988. *The universal airport design system, Rep. I of IV: Granular material characterization*. College Park, MD: Univ. of Maryland.

Yoon, S., U. Balunaini, I. Z. Yildirim, M. Prezzi, and N. Z. Siddiki. 2009. "Construction of an embankment with a fly and bottom ash mixture: Field performance study." *J. Mater. Civ. Eng.* 21 (6): 271–278. https://doi.org/10.1061/(ASCE)0899-1561(2009)21:6(271).

Downloaded from ascelibrary.org by Univ of Witwatersrand on 04/09/25. Copyright ASCE. For personal use only; all rights reserved.